Different methods for RUL prediction considering sensor degradation

Hassan Hachem, Hai Canh Vu, Mitra Fouladirad

Different methods for RUL prediction considering sensor degradation

Hassan Hachem [a], Hai Canh Vu [b], Mitra Fouladirad [c,*]

[a] Troyes University of Technology, France
[b] University Technology of Compiègne, France
[c] Aix Marseille Université, M2P2, Centrale Marseille, France

ARTICLE INFO

Keywords:
System degradation
Sensor degradation
Particle filter
Remaining useful lifetime

ABSTRACT

Predicting the Remaining Useful Lifetime (RUL) of a system has become one of the primary goals of engineering and reliability researchers. RUL prediction is based on the measurement data collected from sensors (e.g. vibration data, temperature data). The collected data is may be inaccurate owing to sensor problems. These problems are often ignored or modeled by a Gaussian noise in most previous work. However, due to various operation circumstances and the aging impact, the sensor itself will ultimately deteriorate and its performance will deteriorate. The Gaussian noise with a constant mean is then not appropriate to fully capture the sensor degradation. In this context, this study focuses on predicting the RUL considering the sensor degradation. For this purpose, a joint model of sensor degradation and system degradation is firstly developed. In this model, the sensor degradation is modeled by Wiener and Gamma processes instead of Gaussian noise. Then, different estimation methods based on the particle filter, a popular model-based technique, were proposed to predict the RUL based on the joint degradation model. To study the performances of our methods, numerical analyzes were carried out. The obtained results confirm the performance and advantages of the proposed methods.

1. Introduction

Predictive Maintenance (PdM) is nowadays one of the most important key technologies of Industry 4.0. The main idea of the PdM is to make maintenance decisions based on the future condition of system/component's health instead of based on the current condition (condition-based maintenance) or on the calendar time (calendar-based maintenance). The future condition is usually quantified by Remaining Useful Lifetime (RUL), i.e. a prediction of the remaining time that the system is able to perform its intended function [1,2]. Compared to the other maintenance strategies, the PdM is theoretically more powerful. It can help to anticipate failures, improve service quality, increase system availability, and reduce significantly maintenance costs. However, the PdM's performance highly depends on the accuracy of the RUL prediction approaches (prognostic approaches) [3].

At the highest level, the prognostic approaches can be divided into two categorizations: Model-driven and Data-driven approaches. Data-driven prediction approach is used when the complexity of the considered system makes it impossible to derive accurate mathematical models or when the knowledge about the system is very limited. In this framework, the prediction process is only based on the historical data collected from sensors. The precision in predicting then depends a lot on the quality and quantity of the collected data [4] . In the literature, a number of data-driven prediction techniques has been developed such as Relevant Vector Machine (RVM) [5], Convolutional Neural Networks (CNN) [6], Long-Short Term Memory Networks (LSTM) [7], etc. It is also possible to propose hybrid prognosis methods combining physical models and monitoring or historical data, where the prognosis results could give very efficient results [8].

A model-driven approach estimates the RUL based on the mathematical models of the considered process/system. The main benefit of this approach is the ability to incorporate physical understanding of the system under observation [9]. Thus predicted results are proper in case when the knowledge about the considered system is sufficient to build accurate and robust system mathematical models. However, in many situations, it is usually impossible to obtain the analytic and high-fidelity models of the systems. To this end, dynamic models with unknown parameters are firstly designed to model the system degradation mechanisms. Then, the historical data are used to estimate the unknown parameters of the dynamic models. The dynamic model-driven approach has been intensively developed and applied in real applications thanks to its ability to model complex process/systems. Note that the approach utilizes the historical data in its prediction process, it cannot be classified into data-driven approach because its performance strongly depends on the designed dynamic models. In this framework, various prediction techniques have been developed in

* Corresponding author.
E-mail address: mitra.FOULADIRAD@univ-amu.fr (M. Fouladirad).

the literature such as techniques relying on stochastic processes properties [10–12], Kalman filter [13,14], Particle filter [15,16]. Among them, particle filters (PFs) are more and more studied and implemented for the prognostics of industrial component/system thanks to their powerful performance and their flexibility in predicting the RUL of systems with non-linear and non-Gaussian data [17–19]. Their main idea is to use a set of samples (particles) with associated weights to represent the state density function. The state estimates are then computed based on these particle and weights. The sequential importance sampling is employed to reduce the number of particles which are required to approximate the state probability distribution. PFs are therefore more efficient than the classical Monte Carlo. Given a number of advantages of PFs as well as of the model-driven approaches, the accuracy of the dynamic model describing the degradation mechanisms plays a critical role for the effective operation of the RUL prediction using model-driven approaches and that of the predictive maintenance. More sophisticated PF are proposed and used in the framework of prognosis where the efficiency in terms of prediction error and computational time goes beyond that of the simple PF [20]. These methods can also be combined by other estimation and inference (machine learning) methods to improve the prognosis quality [21–23].

In the literature, to predict the RUL, the system deterioration is usually modeled by a stochastic process [24–26] such as Gamma process, Wiener process. Unfortunately, deterioration data are not always directly observable and their measurements are subject to sensor errors [27–30]. These errors, additive, proportional or in other forms make the precision of the simple stochastic process models decrease significantly. To improve the performance of RUL prediction based on the noisy degradation data, these sensor errors are usually introduced in the system degradation model as white Gaussian noises [31–34]. Given a field degradation case, the type of sensors used for data collection, the system under consideration and historical data give some hints on whether or not sensors deterioration is possible and plausible. For instance, in case of a train, helicopter or airplane the sensors are embedded and they undergo harsh environmental conditions that is why the degradation in some specific data collection is systematically considered. By using the white Gaussian noises to model the sensor errors, we consider that these errors are stationary (remain unchanged over time). Due to this assumption, these models face a lot of difficulties in real applications. Indeed, sensors as systems can be deteriorated and this deterioration leads to increases of the sensor errors over time [35–42]. Unfortunately, to the best of our knowledge sensor deterioration in the framework of prognosis (RUL prediction) has been scarcely studied [43–45]. For this reason, our objective is to take into account the sensor degradation in the RUL prediction. The main contributions of the paper are then the following:

- Sensor degradation modeling by the different stochastic processes and construct joint system-sensor degradation model;
- Proposition of three PF-based prediction methods in presence of sensor degradation and an additive noise;
- Models parameters estimation embedded with Pf-based RUL estimation through bayesian inference with different prior;
- Sensitivity analysis to model parameters, to sensor degradation, to estimation method and to the prediction method.

The remainder of the paper is as follows. First the joint system and sensor degradation model is presented in Section 2. Afterward, in Section 3, different solutions to predict the RUL based on the particle filters are introduced and their implementation is detailed. A sensitivity analysis and comparison of the solutions for prognosis are carried through numerical examples in Section 5. Finally, some conclusions drawn from this work are shown in Section 6.

2. Problem statement

Let Z_t be the degradation measure at time t defined as follows:

$$Z_t = h(X_t, Y_t, \epsilon) = g(X_t, Y_t) + \epsilon, \tag{1}$$

where X_t and Y_t are the system and sensor degradation level at time t respectively. ϵ is the measurement error, $\epsilon \sim \mathcal{N}(0, \sigma^2)$. This model is inspired by [46,47] where the sensor degradation is additively impacting the degradation measure. Moreover, this model results in investigation based on Kappa X sensor data collected on industrial machine vibration and sensor temperature.

The system is considered ad failed when the degradation level reaches a specific threshold called as failure threshold. Let us denote L the failure threshold. Hence the lifetime of the system is considered as the first time the degradation level exceeds L denoted by T_L defined as follows:

$$T_L = \inf\{t \geqslant 0 : X_t \geqslant L\}. \tag{2}$$

The aim is to predict the system lifetime, all along the system monitoring. In other words, the main objective is to estimated residual lifetime of the system according to observation which is called prognosis. To this end, the Remaining Useful Life (RUL) of the system at each time should be estimated. In the framework of this paper, the remaining useful life is defined as follows:

$$RUL_X(t) = \inf\{h \geqslant 0, X_{t+h} > L \text{ such that } X_t < L\} \tag{3}$$

In sum, the objective is to derive the probability distribution function of T_L and RUL_X based on collected observations during the system lifetime and plan actions accordingly. Since the degradation level of the system and the sensor are not directly observable, in order to predict the system failure, the degradation level estimation is of major importance.

In this paper, as mentioned in the introduction, the degradation phenomenon is considered as random and is modeled by a stochastic process. Due to the uncertainties associated to the observations and the degradation processes, the degradation level estimation induces the degradation level probability density function estimation conditionally to observations. This latter requires the conditional probability derivation which involves numerous integral calculations. As it will be explained in the next sections this difficulty will be bypassed by numerical techniques such as particle filters.

In the following paragraphs, two stochastic processes are considered to model the degradation of the system and the sensor $(X_t)_{t\geq 0}$ and $(Y_t)_{t\geq 0}$.

2.1. Gamma process

Gamma process is a Lévy subordinator (Lévy process with non-decreasing trajectories) which is largely used to model the degradation [48,49] The choice of this process to model the degradation of a system is mainly motivated by a desire to consider systems that cannot improve without maintenance actions. In its homogeneous form the gamma process with shape parameter $\alpha > 0$ and scale parameter $\beta > 0$ is defined as a stochastic process $(G_t)_{t\geqslant 0}$, [49], having the following properties:

- $G_0 = 0$.
- The nonoverlapping increments of $(G_t)_{t\geqslant 0}$ are independent.
- For every $0 < s < t$, the random variable of increment $G_t - G_s$ follows a gamma distribution $Ga(\alpha(t-s), \beta)$. Which is

$$f_{G_t - G_s}(x) = \frac{\beta^{\alpha(t-s)}}{\Gamma(\alpha(t-s))} x^{\alpha(t-s)-1} \exp(-\beta x) \mathbb{1}_{x\geqslant 0}, \tag{4}$$

where $\mathbb{1}_{x\geqslant 0} = 1$ if $x \geqslant 0$ and $\mathbb{1}_{x\geqslant 0} = 0$ otherwise, and $\Gamma(x) = \int_0^\infty x^{\alpha(t-s)-1} e^{-x} dx$.

As mentioned in [49] the cumulative distribution function of the lifetime T_L can be stated as follows:

$$\mathbb{P}(T_L \leq t) = \mathbb{P}(G_t \geqslant L) = \int_{x=L}^{\infty} f_G(x)dx = \frac{\Gamma(\alpha, L\beta)}{\Gamma(\alpha)} \tag{5}$$

2.2. Wiener process

A Wiener process denoted by $(W_t)_{t\geqslant 0}$ is a stochastic process defined as follows:

- $W_0 = 0$.
- The nonoverlapping increments of $(W_t)_{t\geqslant 0}$ are independent.
- For every $0 < s < t$, the random variable of increment $W_t - W_s$ follows a gaussian distribution $\mathcal{N}(m(t) - m(s), \sigma^2(t-s))$ where $m()$ is the drift function and $\sigma > 0$ is the diffusion parameter.

Unlike the Gamma, which offers a monotonous and increasing path of evolution, the Wiener process is capable of giving a non-monotonic model of a random system. This process is widely used as a mathematical object for modeling different random and strongly fluctuating random phenomena, refer to [50,51].

The lifetime T_L has an inverse gaussian distribution with the probability density function:

$$f_{T_L}(t) = \frac{L - W_0}{\sqrt{2\pi\sigma^2(t-t_0)^3}} \exp(-\frac{(L - W_0 - \mu(t-t_0))^2}{2\sigma^2(t-t_0)})\mathbb{1}_{\{t>0\}} \tag{6}$$

3. Degradation level estimation and prognosis by particle filtering

Considering observations $z_1, \dots, z_n$ at observation times $t_1 < \cdots < t_n$ (realizations of $Z_{t_1}, \dots, Z_{t_n}$), the aim is to derive the conditional probability distribution function of the degradation levels X_{t_m} and Y_{t_m} for $t_m \geq t_n$. In other words, the aim is to calculate

$$p_{X_{t_m}|Z_{t_1},\dots,Z_{t_n}}(z_1, \dots, z_n), \quad p_{Y_{t_m}|Z_{t_1},\dots,Z_{t_n}}(z_1, \dots, z_n)$$

or

$$p_{X_{t_1},\dots,X_{t_m}|Z_{t_1},\dots,Z_{t_n}}(z_1, \dots, z_n), \quad p_{Y_{t_1},\dots,Y_{t_m}|Z_{t_1},\dots,Z_{t_n}}(z_1, \dots, z_n)$$

Let be $\mathbf{X} = (X_{t_1}, X_{t_2}, \dots, X_{t_n})$, $\mathbf{Y} = (Y_{t_1}, Y_{t_2}, \dots, Y_{t_n})$ and $\mathbf{Z} = (Z_{t_1}, Z_{t_2}, \dots, Z_{t_n})$. From Bayes rule the following expression can be derived:

$$p_{\mathbf{X},\mathbf{Y}|\mathbf{Z}}(x_1 \dots, x_n, y_1 \dots, y_n) = \frac{p_{\mathbf{Z}|\mathbf{X},\mathbf{Y}}(z_1, \dots, z_n)p_{\mathbf{X},\mathbf{Y}}(x_1, \dots, x_n, y_1, \dots, y_n)}{p_{\mathbf{Z}}(z_1, \dots, z_n)} \tag{7}$$

Since $\mathbf{X}$ and $\mathbf{Y}$ are independent,

$$p_{\mathbf{Z}|\mathbf{X},\mathbf{Y}}(z_1, \dots, z_n) = \prod_{i=1}^{n} p_{Z_{t_i}|X_{t_i},Y_{t_i}}(z_i). \tag{8}$$

Since $(X_t)_{t\geq 0}$ and $(Y_t)_{t\geq 0}$ are Markov processes

$$p_{\mathbf{X},\mathbf{Y}}(x_1, \dots, x_n, y_1, \dots, y_n) = \prod_{i=1}^{n} p_{X_{t_i}|X_{t_{i-1}}}(x_i) \prod_{i=1}^{n} p_{Y_{t_i}|Y_{t_{i-1}}}(y_i) \tag{9}$$

Moreover,

$$p_{\mathbf{Z}}(z_1, \dots, z_n) = \int \cdots \int p_{\mathbf{Z}|\mathbf{X},\mathbf{Y}}(z_1, \dots, z_n)p_{\mathbf{X},\mathbf{Y}}(x_1, \dots, x_n, y_1, \dots, y_n) \times dx_1 \dots dx_n dy_1 \dots dy_n$$

For prognosis, the aim is to estimate the probability density functions of $(X_{t_{n+1}}, \dots, X_{t_{n+m}})$, $(Y_{t_{n+1}}, \dots, Y_{t_{n+m}})$ given the observations $z_1, \dots, z_n$ at observation times $t_1 < \cdots < t_n$ and $t_n \leq t_{n+1} < t_{n+2} < \cdots < t_{n+m}$. In this purpose, first $p_{\mathbf{X},\mathbf{Y}|\mathbf{Z}}$ is derived and then by using the transition probabilities associates to processes $(X_t)_{t\geq 0}$ and $(Y_t)_{t\geq 0}$ the probability density functions of $(X_{t_{n+1}}, \dots, X_{t_{n+m}})$ and $(Y_{t_{n+1}}, \dots, Y_{t_{n+m}})$ are obtained.

Due to presence of a large number of integrals in the denominator of Eq. (7), numerical methods are used to derive this expression. In this paper the conditional density estimation is carried out by using sequential Monte Carlo simulation techniques also known as particle filter (PF), refer to [52]. The Particle filter is the most appropriate approach for non-gaussian and non-linear models, as it is capable of providing arbitrarily posterior probability distribution. PF – also called bootstrap filter [52], Monte Carlo filter [53], or Condensation filter [54] – is a Monte-Carlo based approach that uses a set of particles with associated weights to obtain the posterior probability density of the state with the least variance. The Particle filter estimates sequentially $X = (x_1, x_2, \dots, x_n)$ and $Y = (y_1, \dots, y_n)$ using Eqs. (8) and (9).

Let us consider that the function g defined in Eq. (1) is as follows $g : \mathbb{R} \times \mathbb{R} \to \mathbb{R}$ where $g(x, y) = x + y$. Tn this paper, three degradation estimation and prognosis methods are considered according to

$$Z_t = X_t + Y_t + \epsilon, \tag{10}$$

where X_t and Y_t are the system and sensor degradation level at time t respectively. ϵ is the measurement error, $\epsilon \sim \mathcal{N}(0, \sigma^2)$. The three methods differ in the way they handle the noise and estimate the deterioration state. In the first method, both system and sensor degradations are estimated together by filtering the additive noise. In the second method, first the additive noise is extracted and then the system state is filtered regrading the sensor deterioration as an additive noise. Whereas, in the third method, the sensor deterioration and the additive noise are considered as noise and the deterioration state is filtered.

3.1. First method

Let be $S_t^{(1)} = \begin{pmatrix} X_t \\ Y_t \end{pmatrix}$, therefore,

$$Z_t = (1 \;\; 1)S_t^{(1)} + \epsilon. \tag{11}$$

In the framework of this method, first we shall estimate the conditional probability distribution function of the vector $S_t^{(1)}$ and then derive the marginals of X_t and Y_t. As mentioned before, the conditional probabilities as estimated through particle filter method.

Algorithm 1: First Method

- $k = 1$

Generate N particles x^i using the prior distribution
Generate N particles y^i using the prior distribution

- $k > 1$

while $x_k^i < L, \; \forall i \in [1, N]$ **do**
  Sample: $x_k^i = \pi_X(x_{k-1}^i), y_k^i = \pi_Y(y_{k-1}^i)$
  if $k \leq T$ **then**
    Sample: $w_k^i = \mathbb{P}(Z_k|x_k^i, y_k^i)$
    Estimation: $\hat{x}_k^i = \sum_{i=1}^N w_k^i x_k^i \;\; \hat{y}_k^i = \sum_{i=1}^N w_k^i y_k^i$
    Normalize: $w_k^i = \frac{w_k^i}{\sum w_k^i}$
  $k = k + 1$

In all the algorithms the following points can be highlighted L is the failure threshold and T is the prediction time. There are two phases in the algorithm:

- Phase 1 ($k \in \{1, \dots, T\}$): joint degradation state estimation and weight updating (w_k^i) considering observations (z_k)
- Phase 2 (for $k > T$ and $x_k^i < L$): degradation prediction without updating the weight (w_k^i) because in this phase, there is no new observations. The time that x_k^i exceeds the level L is known (when the while loop stops). For a path x_k^i, the remaining useful lifetime $RUL_i = k$ (the value at which the loop while stops)$-T$(prediction time)

3.2. Second method

Let be $S_t^{(2)} = X_t + Y_t$, therefore,

$$Z_t = S_t^{(2)} + \epsilon, \tag{12}$$

in this method, first the conditional probability distribution function of $S_t^{(2)}$ is derived and then the conditional probability distribution functions of X_t and Y_t are derived. As mentioned before, the conditional probabilities as estimated through particle filter method.

Algorithm 2: Second Method

- $k = 1$

Generate N particles $\hat{x}^i / \hat{y}^i$ using the prior distribution

- $k > 1$

while $\hat{x}_k^i < L,\ \forall i \in [1, N] / \ \hat{y}_k^i < L',\ \forall i \in [1, N]$ **do**
  Sample: $\hat{x}_k^i = \pi_X(\hat{x}_{k-1}^i)$, or $\hat{y}_k^i = \pi_Y(\hat{y}_{k-1}^i)$
  if $k \leq T$ **then**
    Sample: $w_k^i = \mathbb{P}(Z_k|\hat{x}_k^i)$, or $w_k^i = \mathbb{P}(Z_k|\hat{y}_k^i)$
    Estimation: $\hat{x}_k^i = \sum_{i=1}^N w_k^i \hat{x}_k^i$, or $\hat{y}_k^i = \sum_{i=1}^N w_k^i \hat{y}_k^i$
    Normalize: $w_k^i = \frac{w_k^i}{\sum w_k^i}$
  $k = k + 1$

3.3. Third method

Let be $\tilde{\epsilon}_t = Y_t + \epsilon$, therefore,

$$Z_t = X_t + \tilde{\epsilon}_t, \tag{13}$$

In this method, first the conditional probability distribution function of X_t is derived considering $\tilde{\epsilon}_t$ as noise. The conditional probability distribution function of Y_t is derived by the conditional probability distribution of $\tilde{\epsilon}_t$. As in the previous methods, the conditional probabilities as estimated through particle filter method.

Algorithm 3: Third Method

- $k = 1$

Generate N particles x^i / y^i using the prior distribution

- $k > 1$

while $x_k^i < L,\ \forall i \in [1, N]\ /\ y_k^i < L',\ \forall i \in [1, N]$ **do**
  Sample: $x_k^i = \pi_X(x_{k-1}^i)$ or $y_k^i = \pi_Y(y_{k-1}^i)$
  if $k \leq T$ **then**
    Sample: $w_k^i = \mathbb{P}(Z_k|x_k^i)$ or $w_k^i = \mathbb{P}(Z_k|y_k^i)$
    Estimation: $\hat{x}_k^i = \sum_{i=1}^N w_k^i x_k^i$ or $\hat{y}_k^i = \sum_{i=1}^N w_k^i y_k^i$
    Normalize: $w_k^i = \frac{w_k^i}{\sum w_k^i}$
  $k = k + 1$

The prognosis is to define the probabilities ?? which are particular cases of ??

4. Prognosis with unknown parameters

In real-life problems, the true values of degradation parameters are unknown. Hence parameter estimation is essential to predict the RUL for a practical prognosis method. In this section, the parameters of the system degradation model are considered to be unknown. To predict the failure and estimate the RUL the parameters have to be estimated. It is supposed that a prior knowledge on parameters might be available by expert of degradation monitoring or system designers. Therefore, the focus will be on the bayesian estimation framework. Bayesian estimation in the framework of Wiener and gamma process has been largely investigated. Wiener process data fitting has been largely discussed in [55]. Authors in [56] estimates the unknown parameters of a Wiener process in a Bayesian framework through Markov chain Monte Carlo. In [57], Gibbs sampling is used in order to estimate the unknown parameters of the Brownian stress–strength models. The unknown parameter of the Wiener process are estimated and updated through the bootstrap method and Bayesian theorem in [58]. In [59] the parameters of the change-point wiener process model are estimated using a hierarchical Bayesian technique. The Bayesian parameter estimation of a Gamma process is presented in [49]. Authors in [60] deal with unknown gamma process parameters through Approximate Bayesian Computation (ABC). In order to lower the rejection rate of the ABC method, the Markov Chain Monte Carlo is used within the ABC method. Dufresne et al. [61] propose using a conjugate Bayesian analysis with an inverted gamma distribution as the prior for the scale parameter of the gamma process. Gamma process parameter estimation has also been considered in other framework, [32,62].

To avoid the well-known issues related to the difficult elicitation of a prior distribution [63], an objective Bayesian framework can be chosen [64,65]. Especially defended by Clarke [66], a relevant non-informative prior measure $\pi(\theta)$ is Jeffreys' prior. It is basically defined as the square root of the determinant of the Fisher matrix, and is therefore intrinsically linked to the form of the likelihood (see [64] for details). Even though, an informative prior density $\pi(\theta)$ elicitation is rather difficult since it introduces a level of subjectivity within the model, nevertheless, the presence of available information, provided by industrial experts, can sometimes be as much valuable as the observations. Therefore, a clear methodology of prior elicitation must be provided, where the (hyper)parametric model for $\pi(\theta)$ have practical meanings for the practitioners. To our knowledge, no work was published about the elicitation of parametric prior distributions on parameters of gamma processes, in the field of industrial reliability. Most researchers (working in this field or not) considered more willingly gamma distribution themselves as prior structures for non-parametric or semi-parametric intensity models [67–69], or used a nonparametric framework to propose Bayesian estimators of gamma process parameters [70].

Let be $\theta = (\mu_X, \sigma_X, \mu_Y, \sigma_Y)$ the vector of unknown four parameters. Let be π_θ the prior of θ and π_{μ_X}, π_{σ_X}, π_{μ_Y}, π_{σ_X} be the marginals associates to μ_X, σ_X, μ_Y, σ_Y respectively. The parameters are supposed to be independent, therefore, $\pi_\theta(m_1, s_1, m_2, s_2) = \pi_{\mu_X}(m_1)\pi_{\sigma_X}(s_1)\pi_{\mu_Y}(m_2)$ $\pi_{\sigma_X}(s_2)$. The idea is to estimate the parameters by calculating their posterior distributions π^p of θ considering observations $z_1, \ldots, z_n$:

$$\pi^p{}_{\theta|\mathbf{Z}}(\mu_X, \sigma_X, \mu_Y, \sigma_Y) \propto p_{\mathbf{Z}|\theta}(z_1, \ldots, z_n)\pi_\theta(\mu_X, \sigma_X, \mu_Y, \sigma_Y)$$

where

$$p_{\mathbf{Z}|\theta}(z_1, \ldots, z_n) = \int \cdots \int p_{\mathbf{Z}|\mathbf{X},\mathbf{Y},\theta}(z_1, \ldots, z_n) p_{\mathbf{X},\mathbf{Y}|\theta}(x_1, \ldots, x_n, y_1, \ldots, y_n) \times dx_1 \ldots dx_n dy_1 \ldots dy_n$$

In order to derive the posterior distribution of θ filtering techniques should be implemented. In this paper PF is employed to estimate both degradations and the model's parameters. According to [71] in PF, the Bayesian update is processed sequentially with particles having probability information of unknown parameters; when a new measurement is available, the posterior at the previous step is used as the prior information at the current step, and the parameters are updated by multiplying it with the likelihood, this procedure is described below. In Algorithm 4, the estimation and prognosis algorithm is given.

After the parameter estimation and prognosis through PF, the impact of the uncertainty related to parameters on the prognosis results is investigated.

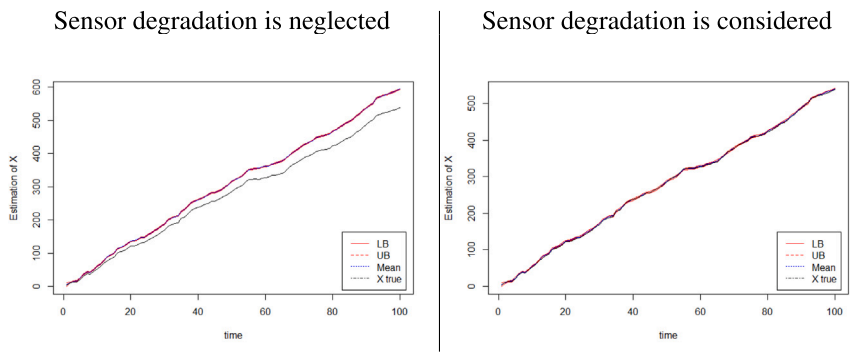

Fig. 1. Estimation of the system degradation at $t = 100$.

Algorithm 4: First Method: State and Parameters Estimation

- $k = 1$

Generate N particles x^i using the prior distribution
Generate N particles y^i using the prior distribution
Generate N particles $\mu^i_{X,k-1}$ using the prior distribution
Generate N particles $\sigma^i_{X,k-1}$ using the prior distribution
Generate N particles $\mu^i_{Y,k-1}$ using the prior distribution
Generate N particles $\sigma^i_{Y,k-1}$ using the prior distribution

- $k > 1$

for $k \in [0, T]$ **do**
  Sample: $x^i_k = \pi_X(x^i_{k-1}, \mu^i_{X,k-1}, \sigma^i_{X,k-1})$ $y^i_k = \pi_Y(y^i_{k-1}, \mu^i_{Y,k-1}, \sigma^i_{Y,k-1})$ $w^i_k = \mathbb{P}(Z_k|x^i_k, y^i_k)$
  Estimation: $\hat{x}^i_k = \sum_{i=1}^N w^i_k x^i_k$ $\hat{y}^i_k = \sum_{i=1}^N w^i_k y^i_k$
  Normalize: $w^i_k = \frac{w^i_k}{\sum w^i_k}$

Table 1
MSE and RMSE of the estimation at $t = 100$.

	MSE	RMSE
Sensor degradation is neglected	1074.056	32.7728
Sensor degradation is considered	3.815926	1.953439

5. Numerical study

5.1. The advantage of sensor degradation consideration

In order to underline the importance of the consideration of sensor degradation, we consider the case where both the system degradation $(X_t)_{t\geq 0}$ and the sensor degradation $(Y_t)_{t\geq 0}$ are modeled by Wiener processes with the following parameters: $\mu_X = 5, \sigma_X = 3, \mu_Y = 0.5, \sigma_Y = 0.3$. In addition, a Gaussian noise $\epsilon_t \sim \mathcal{N}(0,1)$, $\epsilon'_t \sim \mathcal{N}(0,1)$ is considered. We run our PF by using the two following models:

- The sensor degradation is neglected: $Z_t = X_t + \epsilon_t$
- The sensor degradation is considered: $Z_t = X_t + Y_t + \epsilon'_t$

The results are reported in Fig. 1 and Table 1). The obtained results confirm the advantages of taking into account the sensor degradation. The values of MSE and RMSE when the sensor degradation is considered are much more smaller than those when the it is not considered.

5.2. Degradation models

A wastewater treatment plant is utilized in this section to demonstrate the suggested degradation model. In wastewater treatment plants, the activated sludge technique is frequently used to address contaminants. However, in the presence of filamentous bulking, the normal operation of the activated sludge process is frequently hampered. Sludge bulking is mostly caused by filamentous bacterial growth, which may be described as a degrading process [72,73]. In practice, the sludge volume index (SVI) is an empirical measurement that is often employed to characterize the degradation of filamentous sludge bulking. Regrettably, actual numbers are not available. The example we offer is a real-world situation that serves as an illustration. In this paper it is assumed that the SVI follows a Wiener process, or a Gamma process.

Table 2
Models parameters.

Case 1: W-W	μ_X	σ_X	μ_Y	σ_Y
Case 2: G-G	α_X	β_X	α_Y	β_Y
Case 3: G-W	α_X	β_X	μ_X	σ_X

In this section, the performance of the three proposed method works is studied. As mentioned in Section 2, three different cases shall be considered.

- case 1 W-W: Two Wiener processes as the system and the sensor degradation and a gaussian noise.

$$X_t - X_s \sim \mathcal{N}(\mu_X(t-s), \sigma_X^2), \quad Y_t - Y_s \sim \mathcal{N}(\mu_Y(t-s), \sigma_Y^2)$$

- case 2 G-G: Two gamma processes, as the system and the sensor degradation and a gaussian noise.

$$X_t - X_s \sim \Gamma(\alpha_X(t-s), \beta_X), \quad Y_t - Y_s \sim \Gamma(\alpha_Y(t-s), \beta_Y^2)$$

- case 3 G-W: A gamma process for system degradation and a Wiener process for the sensor degradation and a gaussian noise.

$$X_t - X_s \sim \Gamma(\alpha_X(t-s), \beta_X), \quad Y_t - Y_s \sim \mathcal{N}(\mu_Y(t-s), \sigma_Y^2)$$

The model parameters are resumed in Table Table 2. For each case, n observations are generated independently using the model defined in Eq. (1). All runs of PF algorithm consist in generating N particles. Two metrics are utilized to study the quality of the estimate of X_{t_i} and for Y_{t_i}: Mean Square Error (MSE) and Root Mean Square Error (RMSE); that is,

$$MSE = \frac{1}{n}\sum_{i=1}^{n}(X_{t_i} - \hat{X}_{t_i})$$
$$RMSE = \sqrt{MSE}.$$

The parameters setting used in this section is presented in Table 3.

5.3. State estimation with three methods

In this section, first the state estimation through the three methods is illustrated through numerical examples. From Fig. 2, it can be noticed

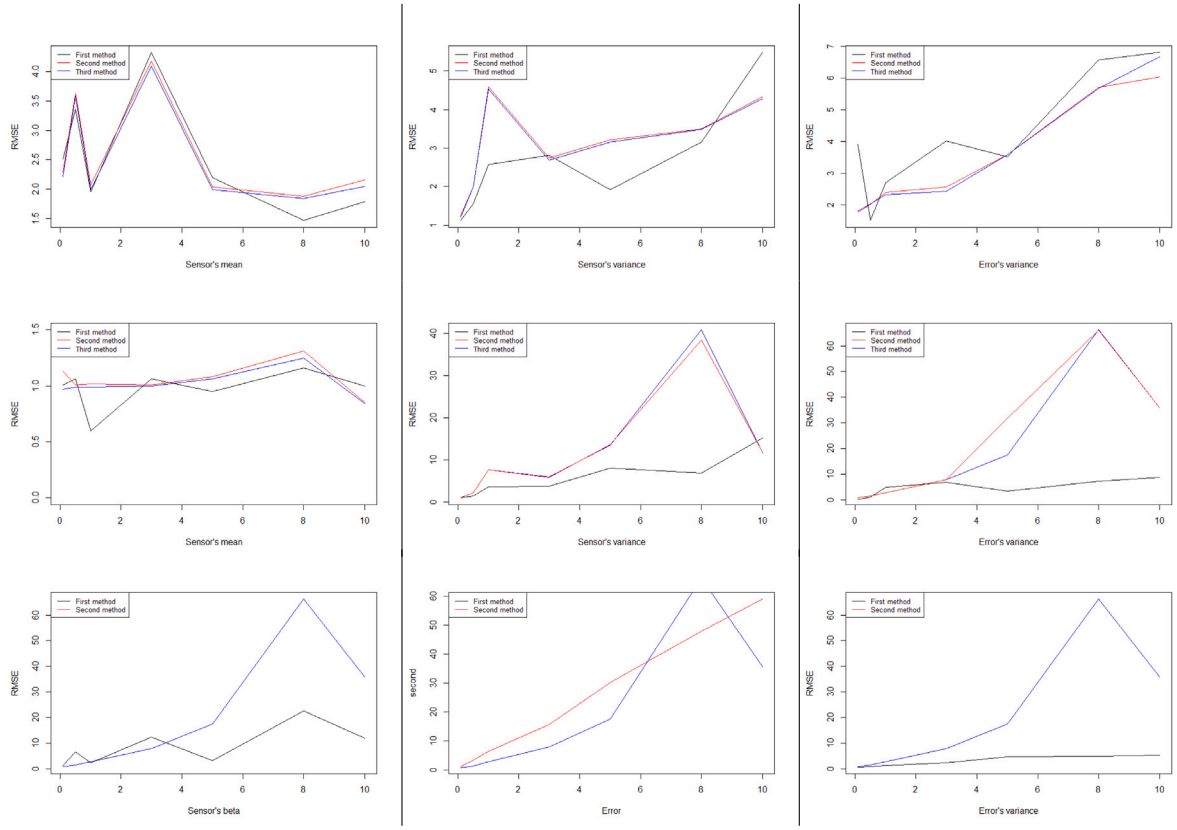

Fig. 2. System state estimation by the three methods for the three different case: first case (top), second case (midst), third case (bottom), at $t = 100$, while varying the sensor's degradation parameters (left and midst) and the error ε variance (right).

Table 3
Parameters setting.

Model 1: W-W	$\mu_X = 5$	$\sigma_X = 3$	$\mu_Y = 0.5$	$\sigma_Y = 0.3$
Model 2: G-W	$\alpha_X = 1$	$\beta_X = 3$	$\mu_X = 0.1$	$\sigma_X = 0.3$
Model 3: G-G	$\alpha_X = 5$	$\beta_X = 1$	$\alpha_Y = 0.5$	$\beta_Y = 0.1$

that the models parameters impact significantly the state estimation and the performance of the three methods. By increasing the variability of the sensor, the performances of the three methods can be very different. Each method seems more suitable for a given scenario

we can see that the error's variance has the greatest influence on the state estimation. For the first and second cases, we cannot say anything about the influence of the sensor's parameter (sometimes we have a smaller RMSE when the mean or the variance is greater). And one can say that the first method is better than the two other. For the third case, we can tell that if the sensor's parameters are smaller the RMSE is smaller and that the first method is better than the second. The sensor's mean does not differentiate the different methods. In sum, a large variability in sensor degradation will not permit an efficient state estimation.

5.4. Prognosis with known degradation parameters

For prognosis the failure threshold L related to the degradation models is set to $L = 800$. First we will study the performance of the proposed method on the different proposed models.

For a given trajectory, a given time t is considered as prognosis time and the degradation before t is considered as the observations (test data) and the crossing time of the trajectory is considered as the real failure time. For Monte Carlo simulations 10 000 trajectories are simulated and for Particle filtering 10 000 particles are generated.

5.4.1. Method performances

First we will study the performance of the proposed method on the different proposed models. The parameters setting is presented in Table 3.

Tables 4–6, give a comparison of the prognosis results obtained through particle filtering obtained by each of the three methods with to results obtained by Monte Carlo Simulations. Monte Carlo simulation focuses on constantly repeating random samples. Hence, after estimating the hidden states until time t (we suppose that our estimations are well estimated – according to the MSEs –) we simulate 10 000 trajectories based on their estimated degradation trend (Wiener/gamma process) until their failure (first time every trajectory exceeds the predefined threshold), from here we get the probability distribution of the RUL.

It can be noticed that prognosis results (RUL estimation at time t) obtained by particle filtering and Monte Carlo Simulations are very close and the mean and median of the estimated RUL are close to the true RUL. The 10% and 90% quantiles lead to acceptable prediction intervals for Case 1 and 2. In contrary for the third model W-G the true RUL is not between the two quantiles.

The same results are depicted in Figs. 3, 4, 5 for a prognosis time $t = 100$. After comparing the first method and the Monte Carlo Simulations, it can be noticed that the histogram' shapes are different.

It should be highlighted that the three methods are very similar in running time.

It should be highlighted that the three methods are very similar in running time.

Table 4
RUL's descriptive statistics of the system using the different the **first estimation method** for the different proposed methods.

Parameters	True RUL	mean	10% quantile	Median	90% quantile
First Model: W-W	50	53.27	47	53	59
Monte Carlo Simulations	50	52.97	47	53	59
Second Model G-W	166	166.16	149	165	182
Monte Carlo Simulations	166	165.3	149	166	182
Third Model G-G	68	62.66	58	62	67
Monte Carlo Simulations	68	62.32	58	62	67

Table 5
RUL's descriptive statistics of the system using the different the **second estimation method** for the different proposed methods.

Parameters	True RUL	mean	10% quantile	Median	90% quantile
First Model	50	51.69	46	52	56
Monte Carlo Simulations	50	52.97	47	53	59
Second Model	166	165.7	149	165	183
Monte Carlo Simulations	166	165.3	149	166	182
Third Model	68	62.76	58	63	67
Monte Carlo Simulations	68	62.32	58	62	67

Table 6
RUL's descriptive statistics of the system using the different the **third estimation method** for the different proposed methods.

Parameters	True RUL	mean	10% quantile	Median	90% quantile
First Model	50	50.66	46	50	56
Monte Carlo Simulations	50	52.97	47	53	59
Second Model	166	165.77	149	167	180
Monte Carlo Simulations	166	165.3	149	166	182
Third Model	68	61.58	57	62	66
Monte Carlo Simulations	68	62.32	58	62	67

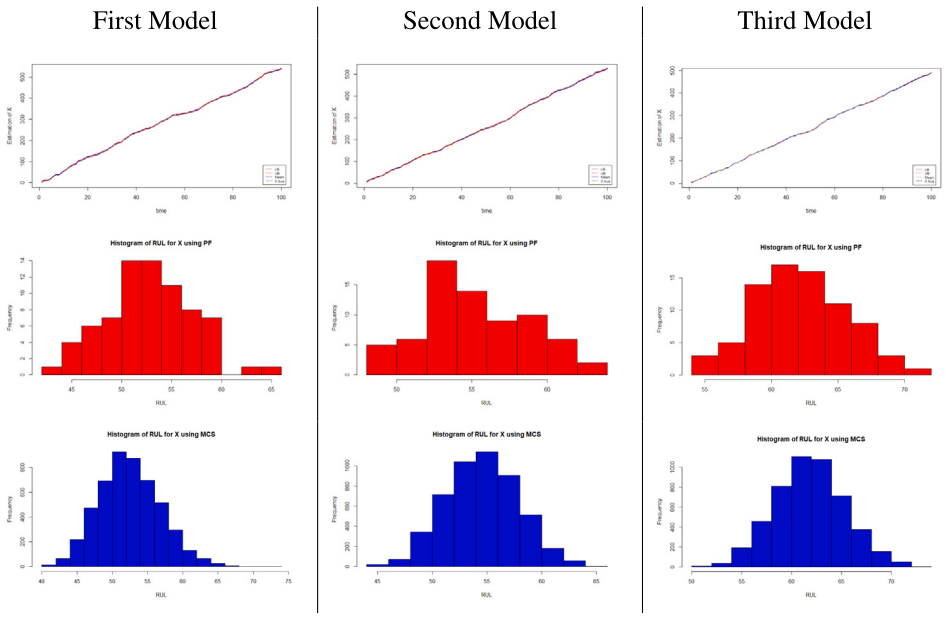

Fig. 3. System state estimation (top), Histogram of system's RUL using the first method (midst) and using Monte Carlo Simulations (bottom) for the different models, at $t = 100$.

5.4.2. *Sensitivity analysis to prognosis time*

The system's RUL is predicted while varying the prognosis time, refer to Figs. 6, 7.

For the first model the results are conservative (the estimation interval bounds are lower than the true failure time), whereas for model 2 the prediction seems very suitable and for the third model the failure prediction is later than the observed values which can induce unavailability costs in the framework of a predictive maintenance.

Considering Tables 7, 8, 9, it can be noticed that the distribution of the RUL obtained by different methods could be very different. However, often the true RUL is in the 90% confidence bound. Therefore, the three methods seem to be all suitable for prognosis even if they seem to be slightly optimistic and predict a rather later failure times.

5.4.3. *Sensitivity analysis to model parameters*

The independent and identically distributed ϵ is generated according to $\mathcal{N}(0, 1)$, for the first two models. The system's RUL is predicted using different parameters. The prognosis time is fixed to $t = 100$.

Unsurprisingly, it can be noticed in Tables 10, 11, and 12, that when the sensor's degradation average trend is slow the state estimation is better. When the sensor's degradation rate is higher an accurate estimation is more difficult and the prognosis results are less precise.

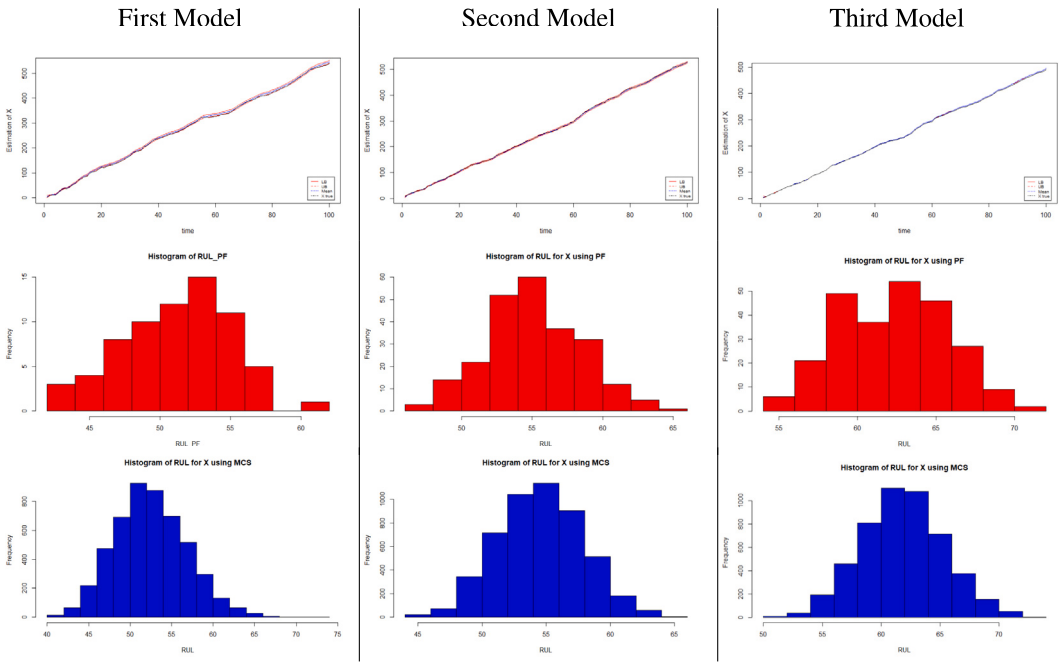

Fig. 4. System state estimation (top), Histogram of system's RUL using the second method (midst) and using Monte Carlo Simulations (bottom) for the different models, at $t = 100$.

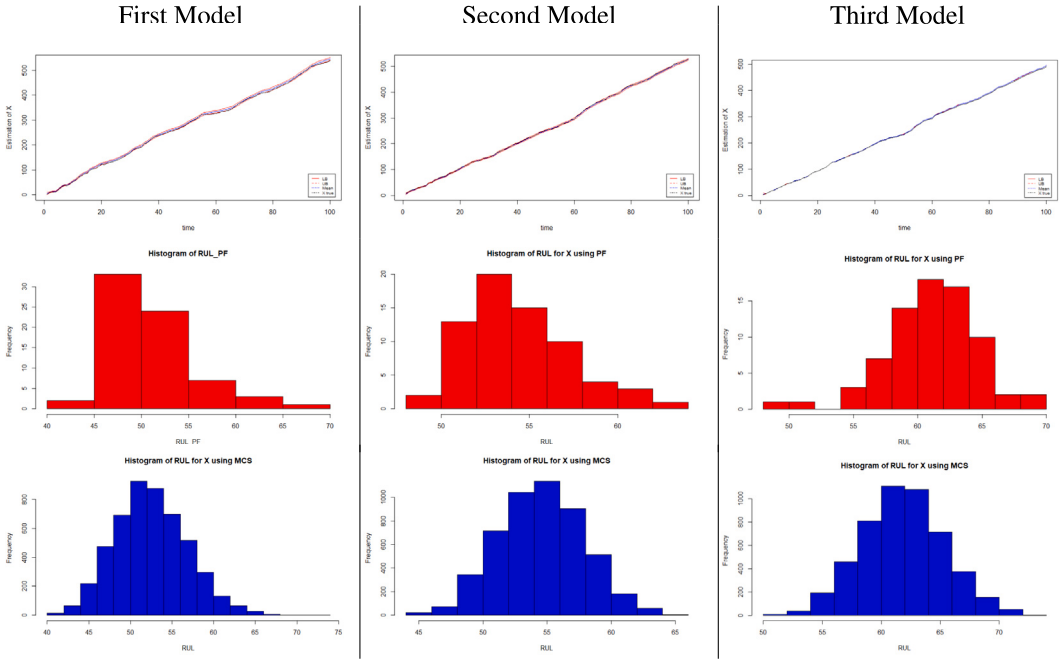

Fig. 5. System state estimation (top), Histogram of system's RUL using the third method (midst) and using Monte Carlo Simulations (bottom) for the different models, at $t = 100$.

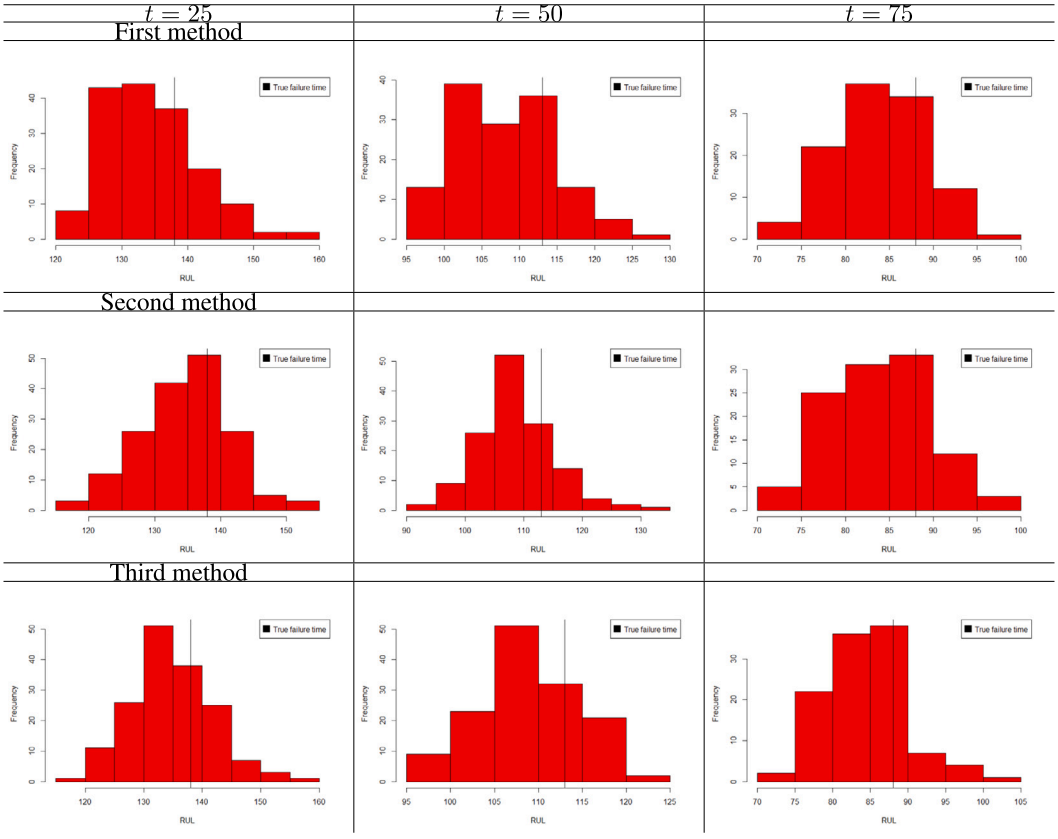

Fig. 6. RUL's histograms of the system with model W-W for different prognosis times.

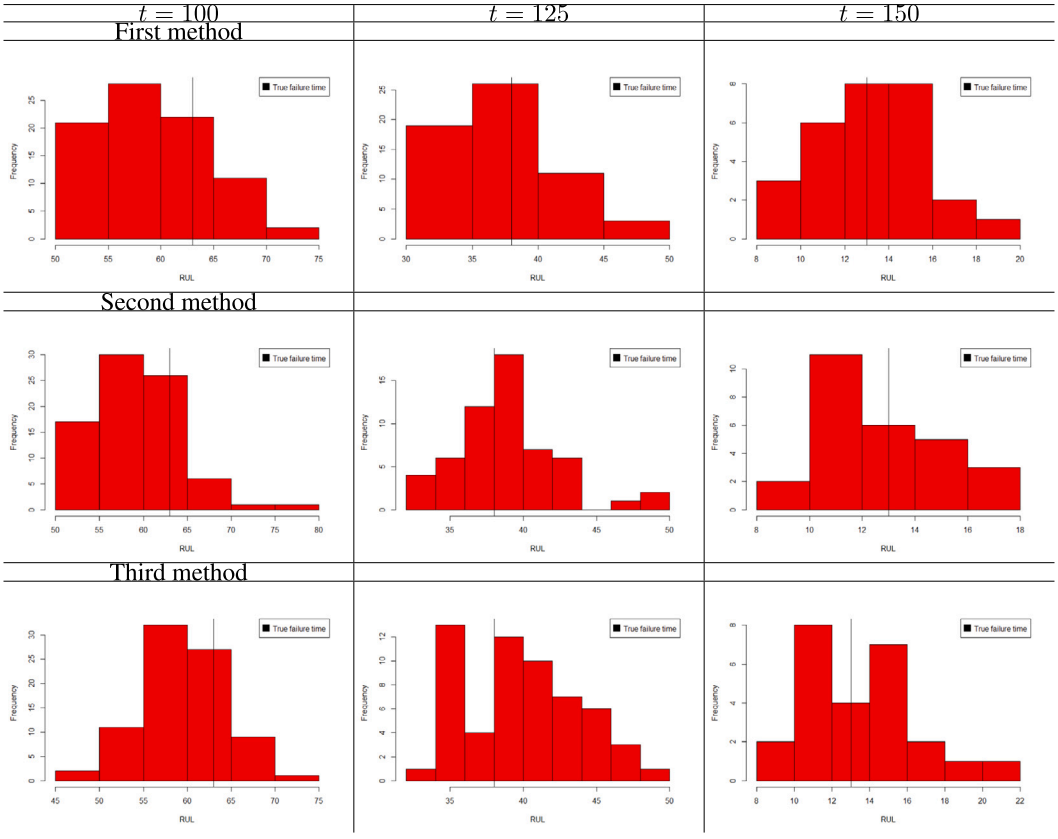

Fig. 7. RUL's histograms of the system with model W-W for different prognosis times.

Table 7
RUL's descriptive statistics of the system with model W-W for different prognosis times.

Prediction time	$t_1 = 50$	$t_2 = 100$	$t_3 = 150$
True RUL	113	63	13
	First method		
Mean	110.35	61.94	14.05
10% quantile	110	60	12
Median	115	64	14
90% quantile	120	65	15
	Second method		
Mean	112.24	62.66	12.04
10% quantile	109	62	11
Median	111	64	14
90% quantile	113	67	16
	Third method		
Mean	110.78	61.54	11.45
10% quantile	108	60	11
Median	111	62	13
90% quantile	113	64	15

Table 8
RUL's descriptive statistics of the system with model G-W for different prognosis times.

Prediction time	$t_1 = 50$	$t_2 = 100$	$t_3 = 150$
True RUL	107	57	7
	First method		
Mean	101.82	60.87	7.33
10% quantile	96	56	6
Median	101	62	8
90% quantile	109	66	9
	Second method		
Mean	101.65	61.6	7.14
10% quantile	96	55	6
Median	105	59	8
90% quantile	108	63	10
	Third method		
Mean	102.98	54.35	7.17
10% quantile	103	55	6
Median	105	58	7
90% quantile	109	63	8

Table 9
RUL's descriptive statistics of the system with model G-G for different prognosis times.

Prediction time	$t_1 = 50$	$t_2 = 100$	$t_3 = 150$
True RUL	220	170	120
	First method		
Mean	220.82	173.98	104.4
10% quantile	210	159	114
Median	215	164	116
90% quantile	220	168	119
	Second method		
Mean	231.23	175.54	116.45
10% quantile	221	163	110
Median	232	173	114
90% quantile	240	182	118
	Third method		
Mean	219.08	173.46	112.54
10% quantile	207	156	112
Median	214	160	116
90% quantile	220	168	119

Table 10
Prognosis sensitivity analysis to model parameters considering Model W-W.

Parameters	True RUL	mean	Confidence interval
First method			
$\mu_X = 1, \sigma_X = 1, \mu_Y = 0.1, \sigma_Y = 0.1$	659	687.32	[655–718]
$\mu_X = 5, \sigma_X = 1, \mu_Y = 0.5, \sigma_Y = 0.1$	62	59.62	[57–62]
$\mu_X = 5, \sigma_X = 3, \mu_Y = 0.5, \sigma_Y = 0.3$	50	53.27	[47–59]
$\mu_X = 5, \sigma_X = 1, \mu_Y = 5, \sigma_Y = 1$	59	57.73	[56–60]
$\mu_X = 1, \sigma_X = 0.5, \mu_Y = 5, \sigma_Y = 1$	683	693.3	[677–709]
Second method			
$\mu_X = 1, \sigma_X = 1, \mu_Y = 0.1, \sigma_Y = 0.1$	659	685.20	[653–719]
$\mu_X = 5, \sigma_X = 1, \mu_Y = 0.5, \sigma_Y = 0.1$	62	61.77	[55–67]
$\mu_X = 5, \sigma_X = 3, \mu_Y = 0.5, \sigma_Y = 0.3$	50	51.69	[46–56]
$\mu_X = 5, \sigma_X = 1, \mu_Y = 5, \sigma_Y = 1$	59	54.52	[52–57]
$\mu_X = 1, \sigma_X = 0.5, \mu_Y = 5, \sigma_Y = 1$	683	679.33	[662–696]
Third method			
$\mu_X = 1, \sigma_X = 1, \mu_Y = 0.1, \sigma_Y = 0.1$	659	685.34	[653–720]
$\mu_X = 5, \sigma_X = 1, \mu_Y = 0.5, \sigma_Y = 0.1$	62	59.89	[58–61]
$\mu_X = 5, \sigma_X = 3, \mu_Y = 0.5, \sigma_Y = 0.3$	50	50.66	[46–56]
$\mu_X = 5, \sigma_X = 1, \mu_Y = 5, \sigma_Y = 1$	59	54.66	[53–57]
$\mu_X = 1, \sigma_X = 0.5, \mu_Y = 5, \sigma_Y = 1$	683	679.22	[663–696]

Table 11
Prognosis sensitivity analysis to model parameters considering the Model G-W.

Parameters	True RUL	mean	Confidence interval
First method			
$\alpha_X = 1, \beta_X = 1, \mu_Y = 0.1, \sigma_Y = 0.1$	707	697.63	[665–734]
$\alpha_X = 5, \beta_X = 1, \mu_Y = 0.5, \sigma_Y = 0.1$	51	55.76	[51–60]
$\alpha_X = 1, \beta_X = 3, \mu_Y = 0.1, \sigma_Y = 0.3$	166	166.16	[149–182]
$\alpha_X = 5, \beta_X = 1, \mu_Y = 5, \sigma_Y = 1$	54	59.18	[54–63]
$\alpha_X = 1, \beta_X = 0.5, \mu_Y = 5, \sigma_Y = 1$	698	701.68	[668–739]
Second method			
$\alpha_X = 1, \beta_X = 1, \mu_Y = 0.1, \sigma_Y = 0.1$	707	697.63	[665–734]
$\alpha_X = 5, \beta_X = 1, \mu_Y = 0.5, \sigma_Y = 0.1$	51	55.76	[51–60]
$\alpha_X = 1, \beta_X = 3, \mu_Y = 0.1, \sigma_Y = 0.3$	166	166.16	[149–182]
$\alpha_X = 5, \beta_X = 1, \mu_Y = 5, \sigma_Y = 1$	54	59.18	[54–63]
$\alpha_X = 1, \beta_X = 0.5, \mu_Y = 5, \sigma_Y = 1$	698	701.68	[668–739]
Third method			
$\alpha_X = 1, \beta_X = 1, \mu_Y = 0.1, \sigma_Y = 0.1$	707	699.68	[666–733]
$\alpha_X = 5, \beta_X = 1, \mu_Y = 0.5, \sigma_Y = 0.1$	51	54.76	[51–59]
$\alpha_X = 1, \beta_X = 3, \mu_Y = 0.1, \sigma_Y = 0.3$	166	165.77	[149–180]
$\alpha_X = 5, \beta_X = 1, \mu_Y = 5, \sigma_Y = 1$	54	56.57	[52–62]
$\alpha_X = 1, \beta_X = 1, \mu_Y = 5, \sigma_Y = 1$	698	696.75	[663–729]

Table 12
Prognosis sensitivity analysis to model parameters considering Model G-G.

Parameters	True RUL	mean	Confidence interval
First method			
$\alpha_X = 1, \beta_X = 1, \alpha_Y = 0.1, \beta_Y = 0.1$	724	714.43	[682–745]
$\alpha_X = 5, \beta_X = 1, \alpha_Y = 0.5, \beta_Y = 0.1$	68	62.66	[58–67]
$\alpha_X = 3, \beta_X = 1, \alpha_Y = 0.3, \beta_Y = 0.1$	165	177.9	[167–188]
Second method			
$\alpha_X = 1, \beta_X = 1, \alpha_Y = 0.1, \beta_Y = 0.1$	724	713.05	[679–745]
$\alpha_X = 5, \beta_X = 1, \alpha_Y = 0.5, \beta_Y = 0.1$	68	62.76	[58–67]
$\alpha_X = 3, \beta_X = 1, \alpha_Y = 0.3, \beta_Y = 0.1$	165	178.16	[168–188]
Third method			
$\alpha_X = 1, \beta_X = 1, \alpha_Y = 0.1, \beta_Y = 0.1$	724	711.86	[678–746]
$\alpha_X = 5, \beta_X = 1, \alpha_Y = 0.5, \beta_Y = 0.1$	68	61.58	[57–66]
$\alpha_X = 3, \beta_X = 1, \alpha_Y = 0.3, \beta_Y = 0.1$	165	176.16	[166–186]

Table 13
Different parameters and their estimation bias.

Case	Parameters	MSE	RMSE
Case 1	$\mu_X = 1$, $\sigma_X = 1$, $\mu_Y = 0.1$ and $\sigma_Y = 0.1$	0.1816273	0.4261775
Case 2	$\mu_X = 5$, $\sigma_X = 1$, $\mu_Y = 0.5$ and $\sigma_Y = 0.1$	2.947386	1.716795
Case 3	$\mu_X = 5$, $\sigma_X = 1$, $\mu_Y = 5$ and $\sigma_Y = 1$	10.18962	3.192118

Table 14
Descriptive statistics for $\hat{\mu}_X$.

Case	μ_X	10% quantile	50% quantile	90% quantile	mean
Case 1	1	0.8768286	0.9928672	1.122852	1.001519
Case 2	5	4.940482	5.132801	5.218659	5.094787
Case 3	5	4.164185	4.542709	5.063029	4.584907

Table 15
Descriptive statistics for $\hat{\sigma}_X$.

Case	σ_X	10% quantile	50% quantile	90% quantile	mean
Case 1	1	0.9058246	0.9848822	1.087124	0.9878635
Case 2	1	0.9067259	0.9807654	1.074041	0.9826182
Case 3	1	2.554637	2.750578	3.00709	2.782533

Fortunately, in these cases even if the prognosis results are more biased, often they are conservative in the sense that they predict the failure before the real failure time which will not induce an unavailability period applying a predictive maintenance based on these results. The 90% confidence bounds proposed by the three methods varies a little bit and it is difficult to conclude which methods leads to the most efficient estimations. In can highlighted that all the estimations methods can be considered as reliable for decision making.

5.5. Prognosis with unknown parameters

As it was pointed out in the previous section that the three methods lead to close prognosis results, in this section only the first method is considered for the prognosis uncertainty investigation. The different prior distributions used for parameter estimation are listed below. In our case $\theta = (\mu_X, \sigma_X, \mu_Y, \sigma_Y)$,

5.5.1. Prior distribution

Non-informative prior: Jeffrey's prior. The Jeffreys prior corresponding to a sample of normally distributed random variables with unknown mean and unknown variance is as follows:

$$\pi(\mu_X, \sigma_X, \mu_Y, \sigma_Y) \propto \frac{1}{\sigma_X^2 \sigma_Y^2}$$

and for a gamma distributed sample

$$\pi(\alpha_X, \beta_X, \alpha_Y, \beta_Y) \propto \frac{1}{\beta_X}\sqrt{\alpha_X \Psi_1(\alpha_X) - 1}\,\frac{1}{\beta_X}\sqrt{\alpha_X \Psi_1(\alpha_X) - 1}$$

where $\Psi_1(.)$ is the trigamma function. For a G-W model,

$$\pi(\alpha_X, \beta_X, \mu_Y, \sigma_Y) \propto \frac{1}{\beta_X \sigma_Y^2}\sqrt{\alpha_X \Psi_1(\alpha_X) - 1}$$

Informative prior. Let Θ_i be the prior information on the value of parameter θ_i. the following priors are defined as follows:

- A uniform prior is defined on each parameters on intervals $[\Theta_i - \eta, \Theta_i + \eta]$, $\eta > 0$ measures the confidence to the expert knowledge.
- A gaussian prior s defined on each parameters as follows: $\mathcal{N}(\eta\Theta_i, p\%\Theta_i)$ where $\eta > 0$, $0 < p \leq 1$ measure the confidence to the expert knowledge.
- A gamma prior with parameters a_i and b_i is defined on each parameters as follows: $\frac{a_i}{b_i} = \eta\Theta_i$ and $\frac{a_i}{b_i^2} = p\%\Theta_i$ where $\eta > 0$, $0 < p \leq 1$ measure the confidence to the expert knowledge.

For each case, 100 observations are generated independently using the W-W model. All runs of PF algorithm consist in generating 200 000 particles (even if the number of the particles increases this would not enhance the estimation). Two metrics are utilized to study the quality of the estimate of X, Y, μ_X, and σ_X: MSE and RMSE. In order to test the robustness of the estimation method different priors and different degradation parameters are considered.

5.5.2. Uncertainty analysis

Non-informative prior: Jeffery's prior. Table 13 gives the parameter estimates bias for three different parameters setting. For each parameters setting in Tables 14 and 15 the quantiles related to the posterior distribution of degradation parameters are given.

Tables 16 and 17 illustrate the impact of the uncertainty of the estimates on the failure time estimation. In 14, case 3, due to large mean and standard deviation associated to the sensor degradation, the observations are very noisy and possibly very far and scattered from the system degradation values. This aspect make the estimation very difficult since it is not possible to separate the both degradations.

Table 16
Impact of the $\hat{\mu}_X$ uncertainty on prognosis results (failure time estimation).

$\mu_X = 1$, $\sigma_X = 1$, $\mu_Y = 0.1$, $\sigma_Y = 0.1$					
Prognosis parameters	failure time	10% quantile	50% quantile	90% quantile	mean
prognosis with true Parameters	672	653	686	720	685.9515
prognosis with 10% quantile	672	742	782	824	782.3445
prognosis with Median	672	657	690	726	690.98
prognosis with 90% quantile	672	583	611	639	611.09
prognosis with Mean	672	652	684	719	684.9574
$\mu_X = 5$, $\sigma_X = 1$, $\mu_Y = 0.5$ $\sigma_Y = 0.1$					
Prognosis parameters	failure time	10% quantile	50% quantile	90% quantile	mean
True Parameters	54	54	58	60	58.2214
10%	54	57	59	61	58.897
Median	54	55	57	59	56.7286
90%	54	54	56	58	55.7942
Mean	54	55	57	59	57.1433
$\mu_X = 5$, $\sigma_X = 1$, $\mu_Y = 5$ $\sigma_Y = 1$					
Prognosis parameters	failure time	10% quantile	50% quantile	90% quantile	mean
True Parameters	71	58	64	71	60.3756
10%	71	69	77	85	77.1104
Median	71	64	70	78	70.6562
90%	71	58	63	70	63.4267
Mean	71	63	70	77	69.9751

Table 17
Impact of the $\hat{\sigma}_X$ uncertainty on prognosis results (failure time estimation).

$\mu_X = 1,\ \sigma_X = 1,\ \mu_Y = 0.1,\ \sigma_Y = 0.1$					
Prognosis parameters	failure time	10% quantile	50% quantile	90% quantile	mean
prognosis with true Parameters	672	653	686	720	685.9515
prognosis with 10% quantile	672	656	685	716	685.9607
prognosis with Median	672	654	686	719	686.2215
prognosis with 90% quantile 672	650	685	723	686.1244	
prognosis with Mean	672	653	686	719	686.2611
$\mu_X = 5,\ \sigma_X = 1,\ \mu_Y = 0.5\ \sigma_Y = 0.1$					
Prognosis parameters	failure time	10% quantile	50% quantile	90% quantile	mean
True Parameters	54	54	58	60	58.2214
10%	54	56	58	60	58.2037
Median	54	56	58	60	58.2331
90%	54	56	58	60	58.1905
Mean	54	56	58	60	58.2251
$\mu_X = 5,\ \sigma_X = 1,\ \mu_Y = 5\ \sigma_Y = 1$					
Prognosis parameters	failure time	10% quantile	50% quantile	90% quantile	mean
True Parameters	71	58	64	71	60.3756
10%	71	59	64	69	64.1327
Median	71	59	64	70	64.2037
90%	71	58	64	71	64.2715
Mean	71	59	64	70	64.2006

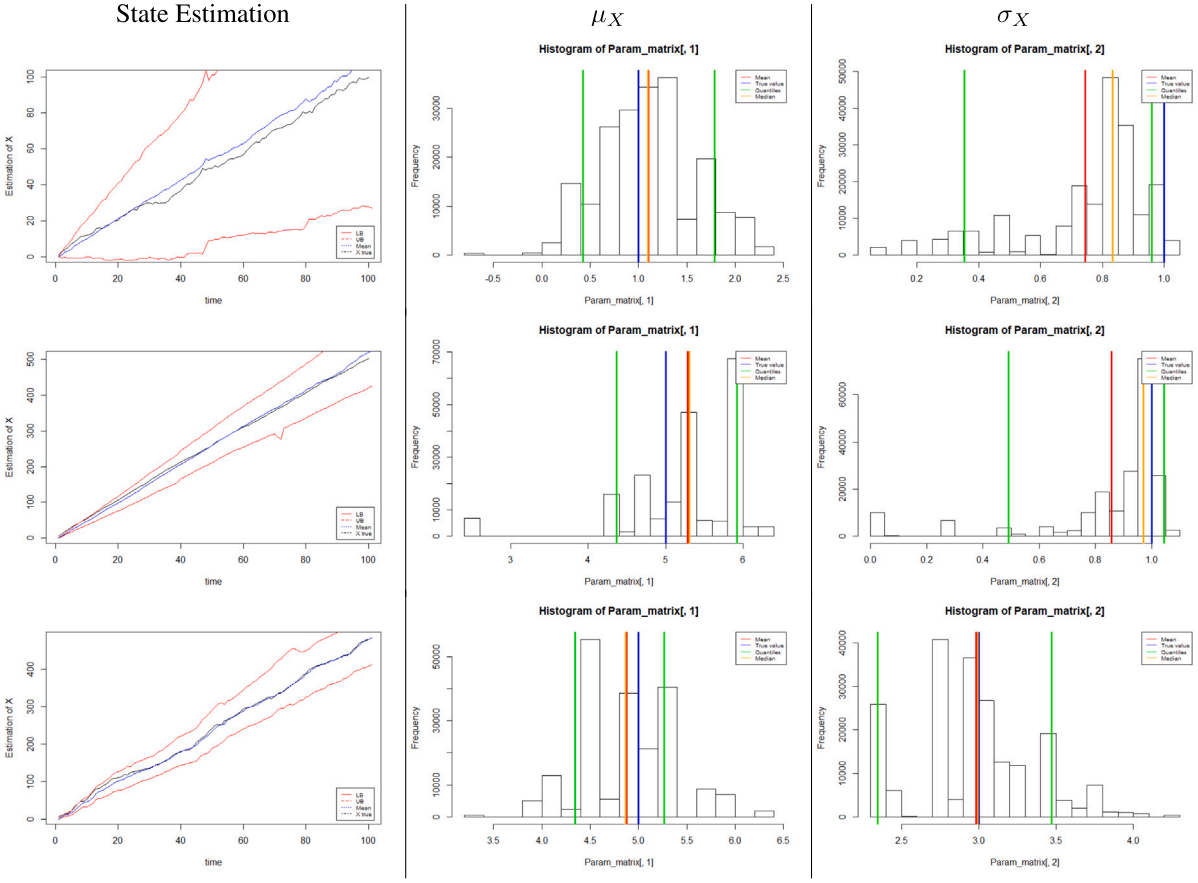

Fig. 8. State estimation for system's degradation(left panel) and histogram of $\hat{\mu}_X$ (middle panel) and $\hat{\sigma}_X$n (right panel) for the different cases.

Table 18
Different parameters and their estimation bias.

Case	Parameters	MSE	RMSE
Case 1	$\mu_X = 1$, $\sigma_X = 1$, $\mu_Y = 0.1$ and $\sigma_Y = 0.1$	0.1636322	0.4045148
Case 2	$\mu_X = 5$, $\sigma_X = 1$, $\mu_Y = 0.5$ and $\sigma_Y = 0.1$	189.9259	13.78136
Case 3	$\mu_X = 5$, $\sigma_X = 1$, $\mu_Y = 5$ and $\sigma_Y = 1$	1387.708	37.25196

Table 19
Descriptive statistics for $\hat{\mu}_X$.

Case	μ_X	10% quantile	50% quantile	90% quantile	mean
Case 1	1	0.7580507	0.8790687	1.035925	0.9067935
Case 2	5	4.570872	5.093009	5.24726	4.904125
Case 3	5	0.745772	5.612498	9.019261	5.174319

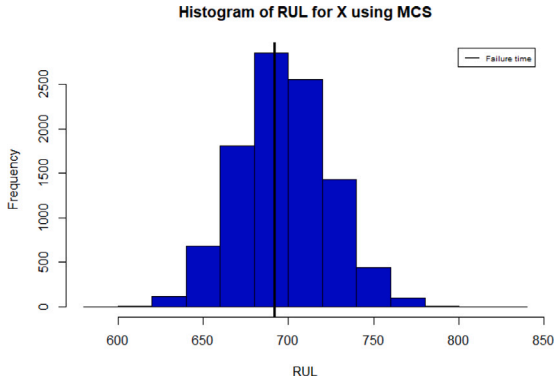

Fig. 9. RUL's histogram while using true parameters.

Uniform distribution. In this part, each parameter has a uniform distribution as prior, with $a = \theta_i - 0.2$, and $b = \theta_i + 0.2$, where θ_i is the true parameter $1 \leq i \leq 4$. In Table 18 the MSE and RMSE associated to state's estimations are given. Tables 19 and 20 represent $\hat{\mu}_X$ and $\hat{\sigma}_X$ the estimates of μ_X and σ_X respectively. Tables 21 and 22 represent the impact of the uncertainty related to estimates on the failure time estimation.

Gaussian distribution. For the gaussian prior, the mean is supposed equal to the Θ_i, $1 \leq i \leq 4$, and the standard deviation is supposed equal to Θ_i. Fig. 8 represents the state estimation regarding different values of the posterior distribution (left panel), and the histograms of both $\hat{\mu}_X$ (middle panel) and $\hat{\sigma}_X$ (right panel) estimation for the different cases. In Figs. 9, 10, 11 the RUL distribution according to the choice of the parameter estimates (mean, mode, quantiles of the posterior distribution) is given. The estimates quality are derived in Table 23. Similarly to the figures, Tables 24, 25, 26, 27 represent the impact of the estimates on the failure time estimation.

Gamma distribution. Tables 28, 29, 30, 31, 32 represent the impact of the estimates on the failure time estimation.

5.6. Empirical conclusions

In sum, the numerical results can be summarized as follows:

- The three state estimations (particle filtration methods) have similar behaviors.
- The prognosis efficiency is more related to noise parameter and sensor degradation parameters. Unsurprisingly, when the sensor degradation is slow or small according to the system degradation, its variations are limited and the noise is negligible the state estimation and therefore the prognosis is very efficient.
- Even if some models seems more sensitive to the noise for prognosis, almost all the prediction intervals include the real failure time.
- In this paper number of particles and simulations are significant that is why the predictions give relatively good results.
- Prognosis results with unknown parameters show acceptable results in comparison with the case when the parameters are known. In other words, the estimation based on a well calibrated priors is efficient.
- The prior elicitation can have a major impact of the prognosis results.
- When the estimation is not efficient (the true RUL is not in the 90% confidence interval) mostly the failure time estimation is earlier than the real failure time which is very conservative and risk averted.

6. Conclusions

See the tables and figures.

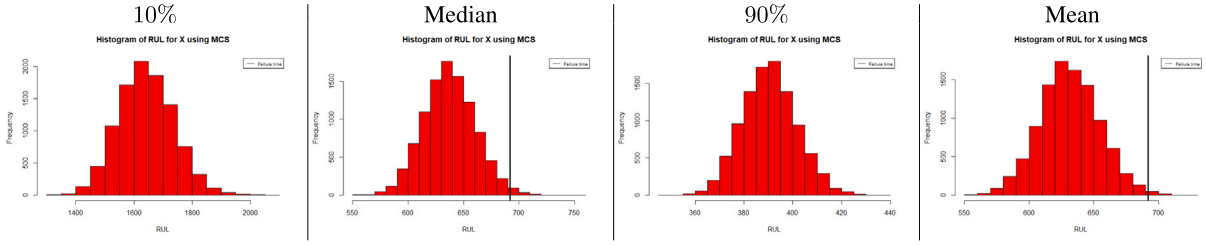

Fig. 10. Impact of the uncertainty around $\hat{\mu}_X$ on RUL's Histograms, for the first case.

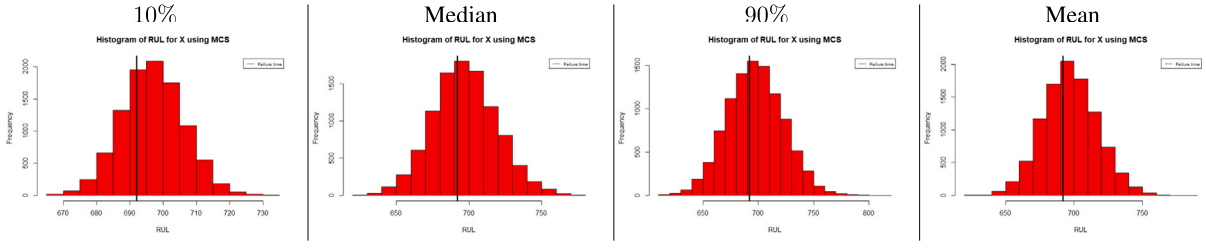

Fig. 11. Impact of the uncertainty around $\hat{\sigma}_X$ on RUL's Histograms, for the first case.

Table 20
Descriptive statistics for $\hat{\sigma}_X$.

Case	σ_X	10% quantile	50% quantile	90% quantile	mean
Case 1	1	0.9914179	1.077884	1.180946	1.078622
Case 2	1	0.8623239	0.9332116	1.065157	0.9583114
Case 3	1	0.2180336	0.9690471	1.458269	0.8847489

Table 21
Impact of the estimates uncertainty on prognosis results (failure time estimation).

$\mu_X = 1,\ \sigma_X = 1,\ \mu_Y = 0.1,\ \sigma_Y = 0.1$					
Prognosis parameters	failure time	10% quantile	50% quantile	90% quantile	mean
prognosis with true Parameters	736	679	712	747	712.9271
prognosis with 10% quantile	736	875	940	993	940.3638
prognosis with Median	736	769	810	853	810.5594
prognosis with 90% quantile	736	656	687	720	687.8317
prognosis with Mean	736	747	785	825	785.7889
$\mu_X = 5,\ \sigma_X = 1,\ \mu_Y = 0.5\ \sigma_Y = 0.1$					
True Parameters	59	54	56	58	56.2946
10%	59	59	61	64	61.5169
Median	59	53	55	57	55.2744
90%	59	52	54	55	53.6421
Mean	59	55	57	59	57.3851
$\mu_X = 5,\ \sigma_X = 1,\ \mu_Y = 5\ \sigma_Y = 1$					
True Parameters	62	59	61	63	61.3302
10%	62	375	409	444	409.2575
Median	62	53	55	56	54.7006
90%	62	33	34	35	34.2289
Mean	62	57	59	61	59.299

Table 22
Impact of the estimates uncertainty on prognosis results (failure time estimation).

Prognosis	failure time	10% quantile	50% quantile	90% quantile	mean
$\mu_X = 1,\ \sigma_X = 1,\ \mu_Y = 0.1,\ \sigma_Y = 0.1$					
prognosis with true Parameters	736	679	712	747	712.9271
prognosis with 10% quantile	736	679	712	747	712.6709
prognosis with Median	736	676	712	750	712.7627
prognosis with 90% quantile	736	672	712	753	712.5708
prognosis with Mean	736	676	712	750	712.5924
$\mu_X = 5,\ \sigma_X = 1,\ \mu_Y = 0.5\ ,\ \sigma_Y = 0.1$					
prognosis with True Parameters	59	54	56	58	56.2946
prognosis with 10%	59	55	56	58	56.2691
prognosis with Median	59	55	56	58	56.2745
prognosis with 90%	54	56	58	56.2563	
prognosis with Mean	59	54	56	58	56.2917
$\mu_X = 5,\ \sigma_X = 1,\ \mu_Y = 5,\ \sigma_Y = 1$					
prognosis with True Parameters	62	59	61	63	61.3302
prognosis with 10%	62	59	61	63	61.3372
prognosis with Median	62	59	61	64	61.4084
prognosis with 90%	62	59	61	64	61.4084
prognosis with Mean	62	60	61	63	61.3238

Table 23
Different parameters and their estimation bias.

Case	Parameters	MSE	RMSE
Case 1	$\mu_X = 1,\ \sigma_X = 1,\ \mu_Y = 0.1$ and $\sigma_Y = 0.1$	35.73929	5.978235
Case 2	$\mu_X = 5,\ \sigma_X = 1,\ \mu_Y = 0.5$ and $\sigma_Y = 0.1$	72.30748	8.503381
Case 3	$\mu_X = 5,\ \sigma_X = 3,\ \mu_Y = 0.5$ and $\sigma_Y = 0.3$	352.4073	18.77251

Table 24
Descriptive statistics for $\hat{\mu}_X$.

Case	μ_X	10% quantile	50% quantile	90% quantile	mean
Case 1	1	0.4250019	1.094191	1.783664	1.104165
Case 2	5	4.369105	5.305121	5.925364	5.285071
Case 3	5	4.345103	4.862624	5.26638	4.876163

Table 25
Descriptive statistics for $\hat{\sigma}_X$.

Case	σ_X	10% quantile	50% quantile	90% quantile	mean
Case 1	1	0.352806	0.832604	0.9597264	0.7447275
Case 2	1	0.4902292	0.9708101	1.043863	0.8574143
Case 3	1	2.34572	2.9931	3.470325	2.787552

Table 26
Impact of the $\hat{\mu}_X$ uncertainty on prognosis results (failure time estimation).

Prognosis	failure time	10% quantile	50% quantile	90% quantile	mean
$\mu_X = 1,\ \sigma_X = 1,\ \mu_Y = 0.1,\ \sigma_Y = 0.1$					
prognosis with true Parameters	692	664	697	733	697.8123
prognosis with 10% quantile	692	1522	1639	1763	1641.747
prognosis with Median	692	608	637	668	637.8131
prognosis with 90% quantile	692	377	391	406	391.0232
prognosis with Mean	692	602	631	663	631.7821
$\mu_X = 5,\ \sigma_X = 1,\ \mu_Y = 0.5\ \sigma_Y = 0.1$					
prognosis with True Parameters	54	54	58	60	58.2214
prognosis with 10% quantile	66	71	73	76	73.2336
prognosis with Median	66	59	60	62	60.4478
prognosis with 90% quantile	66	53	54	56	54.1285
prognosis with Mean	66	51	61	62	60.6424
$\mu_X = 5,\ \sigma_X = 1,\ \mu_Y = 5\ \sigma_Y = 1$					
prognosis with True Parameters	71	58	64	71	60.3756
prognosis with 10% quantile	53	53	59	66	59.3969
prognosis with Median	53	48	53	59	53.0531
prognosis with 90% quantile	53	44	49	54	49.0761
prognosis with Mean	53	48	53	59	53.1118

Table 27
Impact of $\hat{\sigma}_X$ uncertainty on prognosis results (failure time estimation).

Prognosis	failure time	10% quantile	50% quantile	90% quantile	mean
$\mu_X = 1,\ \sigma_X = 1,\ \mu_Y = 0.1,\ \sigma_Y = 0.1$					
prognosis with true Parameters	692	664	697	733	697.8123
prognosis with 10% quantile	692	685	697	709	697.2942
prognosis with Median	692	670	697	726	697.6191
prognosis with 90% quantile	692	666	698	730	697.7786
prognosis with Mean	692	673	697	723	697.4345
$\mu_X = 5,\ \sigma_X = 1,\ \mu_Y = 0.5\ \sigma_Y = 0.1$					
prognosis with True Parameters	54	54	58	60	58.2214
prognosis with 10% quantile	66	63	64	65	64.0485
prognosis with Median	66	62	64	66	64.0963
prognosis with 90% quantile	66	62	64	66	64.102
prognosis with Mean	66	62	64	66	64.0426
$\mu_X = 5,\ \sigma_X = 1,\ \mu_Y = 5\ \sigma_Y = 1$					
prognosis with True Parameters	71	58	64	71	60.3756
prognosis with 10% quantile	53	47	52	56	51.6661
prognosis with Median	53	46	52	57	51.7567
prognosis with 90% quantile	53	46	51	58	51.7023
prognosis with Mean	53	47	52	57	51.6438

Table 28
Different parameters and their estimation bias.

Case	Parameters	MSE	RMSE
Case 1	$\mu_X = 1,\ \sigma_X = 1,\ \mu_Y = 0.1$ and $\sigma_Y = 0.1$	1.200493	1.09567
Case 2	$\mu_X = 5,\ \sigma_X = 1,\ \mu_Y = 0.5$ and $\sigma_Y = 0.1$	7.961347	2.821586
Case 3	$\mu_X = 5,\ \sigma_X = 3,\ \mu_Y = 0.5$ and $\sigma_Y = 0.3$	21.59796	4.647361

Table 29
Descriptive statistics for $\hat{\mu}_X$.

Case	μ_X	10% quantile	50% quantile	90% quantile	mean
Case 1	1	0.7262281	0.8917344	1.018496	0.872597
Case 2	5	4.634436	4.888351	5.063083	4.868262
Case 3	5	4.366648	4.907286	5.195143	4.817564

Table 30
Descriptive statistics for $\hat{\sigma}_X$.

Case	σ_X	10% quantile	50% quantile	90% quantile	mean
Case 1	1	0.940619	1.064352	1.159528	1.053191
Case 2	1	0.9410168	0.9966623	1.087922	1.000278
Case 3	1	2.97348	3.228283	3.44022	3.211805

Table 31
Impact of $\hat{\mu}_X$ on prognosis results (failure time estimation).

Prognosis	failure time	10% quantile	50% quantile	90% quantile	mean
$\mu_X = 1,\ \sigma_X = 1,\ \mu_Y = 0.1,\ \sigma_Y = 0.1$					
prognosis with true parameters	682	669	702	736	702.0841
prognosis with 10% quantile	682	670	702	734	701.8035
prognosis with median	682	666	701	738	701.8481
prognosis with 90% quantile	682	662	702	743	702.3454
prognosis with Mean	682	669	702	737	702.515
$\mu_X = 5,\ \sigma_X = 1,\ \mu_Y = 0.5\ \sigma_Y = 0.1$					
prognosis with true parameters	57	57	59	61	58.7866
prognosis with 10% quantile	57	57	59	61	58.7778
prognosis with median	57	57	59	61	58.8111
prognosis with 90% quantile	57	57	59	61	58.8343
prognosis with mean	57	57	59	61	58.823
$\mu_X = 5,\ \sigma_X = 1,\ \mu_Y = 5\ \sigma_Y = 1$					
prognosis with true Parameters	60	55	60	66	60.3756
prognosis with 10% quantile	60	55	60	66	60.3446
prognosis with median	60	54	60	67	60.4023
prognosis with 90% quantile	60	54	60	67	60.4511
prognosis with mean	60	54	60	67	60.2409

Table 32
Impact of the $\hat{\sigma}_X$ uncertainty on prognosis results (failure time estimation).

Prognosis	failure time	10% quantile	50% quantile	90% quantile	mean
$\mu_X = 1,\ \sigma_X = 1,\ \mu_Y = 0.1,\ \sigma_Y = 0.1$					
prognosis with true parameters	682	669	702	736	702.0841
prognosis with 10% quantile	682	670	702	734	701.8035
prognosis with median	682	666	701	738	701.8481
prognosis with 90% quantile	682	662	702	743	702.3454
prognosis with Mean	682	669	702	737	702.515
$\mu_X = 5,\ \sigma_X = 1,\ \mu_Y = 0.5\ \sigma_Y = 0.1$					
prognosis with true parameters	57	57	59	61	58.7866
prognosis with 10% quantile	57	57	59	61	58.7778
prognosis with median	57	57	59	61	58.8111
prognosis with 90% quantile	57	57	59	61	58.83433
prognosis with mean	57	57	59	61	58.823
$\mu_X = 5,\ \sigma_X = 1,\ \mu_Y = 5\ \sigma_Y = 1$					
prognosis with true Parameters	60	55	60	66	60.3756
prognosis with 10% quantile	60	55	60	66	60.3446
prognosis with median	60	54	60	67	60.4023
prognosis with 90% quantile	60	54	60	67	60.4511
prognosis with mean	60	54	60	67	60.2409

CRediT authorship contribution statement

Hassan Hachem: Investigation. **Hai Canh Vu:** Writing – original draft, Validation, Supervision, Methodology, Formal analysis, Conceptualization. **Mitra Fouladirad:** Writing – review & editing, Writing – original draft, Validation, Supervision, Methodology, Conceptualization.

Declaration of competing interest

On behalf of all the authors declare that there is no conflict of interest in publishing this paper.

Data availability

No data was used for the research described in the article.

Acknowledgments

The authors would like to thank the valuable financial support of the European Regional Development Fund (FEDER) and the Ministry of Higher Education, Research and Innovation of France during this research. All authors approved the version of the manuscript to be published.

References

[1] Bérenguer C, Martinez MJJ, et al. From Deterioration Modeling to Remaining Useful Life Control: A comprehensive framework for post-prognosis decision-making applied to friction drive systems [Ph.D. thesis], Université Grenoble Alpes (ComUE); 2018.

[2] Zio E. Prognostics and Health Management (PHM): Where are we and where do we (need to) go in theory and practice. Reliab Eng Syst Saf 2022;218:108119.

[3] Compare M, Antonello F, Pinciroli L, Zio E. A general model for life-cycle cost analysis of condition-based maintenance enabled by PHM capabilities. Reliab Eng Syst Saf 2022;224:108499.

[4] Aizpurua J, Stewart B, McArthur S, Penalba M, Barrenetxea M, Muxika E, et al. Probabilistic forecasting informed failure prognostics framework for improved RUL prediction under uncertainty: A transformer case study. Reliab Eng Syst Saf 2022;226:108676.

[5] Wang X, Jiang B, Lu N. Adaptive relevant vector machine based RUL prediction under uncertain conditions. ISA Trans 2019;87:217–24.

[6] Yang B, Liu R, Zio E. Remaining useful life prediction based on a double-convolutional neural network architecture. IEEE Trans Ind Electron 2019;66(12):9521–30.

[7] Zhang H, Zhang Q, Shao S, Niu T, Yang X. Attention-based LSTM network for rotatory machine remaining useful life prediction. IEEE Access 2020;8:132188–99.

[8] Chen J, Yuan S, Sbarufatti C, Jin X. Dual crack growth prognosis by using a mixture proposal particle filter and on-line crack monitoring. Reliab Eng Syst Saf 2021;215:107758.

[9] Xu Y, Kohtz S, Boakye J, Gardoni P, Wang P. Physics-informed machine learning for reliability and systems safety applications: State of the art and challenges. Reliab Eng Syst Saf 2022;108900.

[10] Wen Y, Wu J, Das D, Tseng T-LB. Degradation modeling and RUL prediction using Wiener process subject to multiple change points and unit heterogeneity. Reliab Eng Syst Saf 2018;176:113–24.

[11] Lei Y, Li N, Lin J. A new method based on stochastic process models for machine remaining useful life prediction. IEEE Trans Instrum Meas 2016;65(12):2671–84.

[12] Lin J, Liao G, Chen M, Yin H. Two-phase degradation modeling and remaining useful life prediction using nonlinear wiener process. Comput Ind Eng 2021;160:107533.

[13] Le Son K, Fouladirad M, Barros A, Levrat E, Iung B. Remaining useful life estimation based on stochastic deterioration models: A comparative study. Reliab Eng Syst Saf 2013;112:165–75.

[14] Saha B, Goebel K, Poll S, Christophersen J. Prognostics methods for battery health monitoring using a Bayesian framework. IEEE Trans Instrum Meas 2009;58(2):291–6.

[15] Zhang L, Mu Z, Sun C. Remaining useful life prediction for lithium-ion batteries based on exponential model and particle filter. IEEE Access 2018;6:17729–40.

[16] Banerjee A, Putcha C, Gupta SK. Particle filter based prognostic approach for automotive motor. In: 2021 3rd world symposium on artificial intelligence. IEEE; 2021, p. 103–6.

[17] An D, Choi J-H, Kim NH. Prognostics 101: A tutorial for particle filter-based prognostics algorithm using matlab. Reliab Eng Syst Saf 2013;115:161–9.

[18] Zio E, Peloni G. Particle filtering prognostic estimation of the remaining useful life of nonlinear components. Reliab Eng Syst Saf 2011;96(3):403–9.

[19] Wang Y, Peng Y, Chow TW. Adaptive particle filter-based approach for RUL prediction under uncertain varying stresses with application to HDD. IEEE Trans Ind Inf 2021.

[20] Lin Y-H, Jiao X-L. Adaptive kernel auxiliary particle filter method for degradation state estimation. Reliab Eng Syst Saf 2021;211:107562.

[21] Chang Y, Fang H. A hybrid prognostic method for system degradation based on particle filter and relevance vector machine. Reliab Eng Syst Saf 2019;186:51–63.

[22] Li S, Fang H, Shi B. Remaining useful life estimation of lithium-ion battery based on interacting multiple model particle filter and support vector regression. Reliab Eng Syst Saf 2021;210:107542.

[23] Zang Y, Shangguan W, Cai B, Wang H, Pecht MG. Hybrid remaining useful life prediction method. A case study on railway D-cables. Reliab Eng Syst Saf 2021;213:107746.

[24] Kahle W, Mercier S, Paroissin C. Degradation processes in reliability. John Wiley & Sons; 2016.

[25] Shahraki AF, Yadav OP, Liao H. A review on degradation modelling and its engineering applications. Int J Perform Eng 2017;13(3):299.

[26] Yu W, Tu W, Kim IY, Mechefske C. A nonlinear-drift-driven Wiener process model for remaining useful life estimation considering three sources of variability. Reliab Eng Syst Saf 2021;212:107631.

[27] Whitmore G. Estimating degradation by a Wiener diffusion process subject to measurement error. Lifetime Data Anal 1995;1(3):307–19.

[28] Elsayed E, Liao H. A geometric Brownian motion model for field degradation data. Int J Mater Prod Technol 2004;20(1–3):51–72.

[29] Xu X, Tang S, Yu C, Xie J, Han X, Ouyang M. Remaining useful life prediction of lithium-ion batteries based on wiener process under time-varying temperature condition. Reliab Eng Syst Saf 2021;214:107675.

[30] Ding N, Li H, Xin Q, Wu B, Jiang D. Multi-source domain generalization for degradation monitoring of journal bearings under unseen conditions. Reliab Eng Syst Saf 2023;230:108966.

[31] Ye Z-S, Wang Y, Tsui K-L, Pecht M. Degradation data analysis using Wiener processes with measurement errors. IEEE Trans Reliab 2013;62(4):772–80.

[32] Lu D, Pandey MD, Xie W-C. An efficient method for the estimation of parameters of stochastic gamma process from noisy degradation measurements. Proc Inst Mech Eng O 2013;227(4):425–33.

[33] Hao S, Yang J, Berenguer C. Degradation analysis based on an extended inverse Gaussian process model with skew-normal random effects and measurement errors. Reliab Eng Syst Saf 2019;189:261–70.

[34] Pan Y, Hong R, Chen J, Singh J, Jia X. Performance degradation assessment of a wind turbine gearbox based on multi-sensor data fusion. Mech Mach Theory 2019;137:509–26.

[35] Sun J, Zuo H, Wang W, Pecht MG. Prognostics uncertainty reduction by fusing on-line monitoring data based on a state-space-based degradation model. Mech Syst Signal Process 2014;45(2):396–407.

[36] Liu Q, Wang Z, He X, Ghinea G, Alsaadi FE. A resilient approach to distributed filter design for time-varying systems under stochastic nonlinearities and sensor degradation. IEEE Trans Signal Process 2016;65(5):1300–9.

[37] Liu B, Do P, Iung B, Xie M. Stochastic filtering approach for condition-based maintenance considering sensor degradation. IEEE Trans Autom Sci Eng 2019;17(1):177–90.

[38] Li Z, Zhang Y, Wang C. A sensor-driven structural health prognosis procedure considering sensor performance degradation. Struct Infrastruct Eng 2013;9(8):764–76.

[39] Zhang J-X, Si X-S, Du D-B, Hu C-H. Specification analysis of the deteriorating sensor for required lifetime prognostic performance. Microelectron Reliab 2018;85:71–83.

[40] Salehpour Oskouei F, Pourgol-Mohammad M. Degradation evaluation on sensor network optimization in fault diagnosis process. In: ASME international mechanical engineering congress and exposition, vol. 57571. American Society of Mechanical Engineers; 2015, V014T08A019.

[41] Ma S-L, Jiang S-F, Li J. Structural damage detection considering sensor performance degradation and measurement noise effect. Measurement 2019;131:431–42.

[42] Chen Z, Yang C, Peng T, Dan H, Li C, Gui W. A cumulative canonical correlation analysis-based sensor precision degradation detection method. IEEE Trans Ind Electron 2018;66(8):6321–30.

[43] Wang D, Huang K, Liu W, Lin Z, Wang Y. OBD system oxygen sensor degradation monitoring and mechanism analysis. In: 2011 third international conference on measuring technology and mechatronics automation, vol. 2. IEEE; 2011, p. 740–4.

[44] Mukhopadhyay K, Liu B, Bedford T, Finkelstein M. Remaining lifetime of degrading systems continuously monitored by degrading sensors. Reliab Eng Syst Saf 2023;231:109022.

[45] Liu Y, Wang Z, Liu C, Coombes M, Chen W-H. A novel algorithm for quantized particle filtering with multiple degrading sensors: Degradation estimation and target tracking. IEEE Trans Ind Inf 2022;19(4):5830–8.

[46] Mukhopadhyay K, Liu B, Bedford T, Finkelstein M. Remaining lifetime of degrading systems continuously monitored by degrading sensors. Reliab Eng Syst Saf 2022;109022.

[47] He K, Sun Q, Xie M, Kuo W. Sequential Bayesian planning for accelerated degradation tests considering sensor degradation. IEEE Trans Reliab 2022.

[48] Abdel-Hameed M. A gamma wear process. IEEE Trans Reliab 1975;24(2):152–3.

[49] van Noortwijk JM. A survey of the application of gamma processes in maintenance. Reliab Eng Syst Saf 2009;94(1):2–21.

[50] Platen E. A benchmark approach to finance. Math Finance 2006;16(1):131–51.

[51] Platen E, Heath D. A benchmark approach to quantitative finance. Springer Science & Business Media; 2006.

[52] Gordon NJ, Salmond DJ, Smith AF. Novel approach to nonlinear/non-Gaussian Bayesian state estimation. In: IEE proceedings F (Radar and signal processing), vol. 140–2. IET; 1993, p. 107–13.

[53] Kitagawa G. Monte Carlo filter and smoother for non-Gaussian nonlinear state space models. J Comput Graph Stat 1996;5(1):1–25.

[54] MacCormick J, Blake A. A probabilistic exclusion principle for tracking multiple objects. Int J Comput Vis 2000;39(1):57–71.

[55] Zhang Z, Si X, Hu C, Lei Y. Degradation data analysis and remaining useful life estimation: A review on Wiener-process-based methods. European J Oper Res 2018;271(3):775–96.

[56] Hao H, Su C. A Bayesian framework for reliability assessment via Wiener process and MCMC. Math Probl Eng 2014;2014.

[57] Basu S, Lingham RT. Bayesian estimation of system reliability in Brownian stress-strength models. Ann Inst Statist Math 2003;55(1):7–19.

[58] Liu T, Sun Q, Feng J, Pan Z, Huangpeng Q. Residual life estimation under time-varying conditions based on a Wiener process. J Stat Comput Simul 2017;87(2):211–26.

[59] Wang P, Tang Y, Bae SJ, He Y. Bayesian analysis of two-phase degradation data based on change-point Wiener process. Reliab Eng Syst Saf 2018;170:244–56.

[60] Hazra I, Pandey MD, Manzana N. Approximate Bayesian computation (ABC) method for estimating parameters of the gamma process using noisy data. Reliab Eng Syst Saf 2020;198:106780.

[61] Dufresne F, Gerber HU, Shiu ES. Risk theory with the gamma process. ASTIN Bull: J IAA 1991;21(2):177–92.

[62] Bousquet N, Fouladirad M, Grall A, Paroissin C. Bayesian gamma processes for optimizing condition-based maintenance under uncertainty. Appl Stoch Models Bus Ind 2015;31(3):360–79.

[63] Robert C. The Bayesian choice: A decision theoretic motivation. Springer Verlag New York; 2004.

[64] Kass RE WL. The selection of prior distributions by formal rules. J Amer Statist Assoc 1996;91:1343–70.

[65] Lin X CB. Information conversion, effective samples, and parameter size. IEEE Trans Inf Theory 2007;53:4438–56.
[66] Clarke B. Implications of reference priors for prior information and for sample size. J Amer Statist Assoc 1996;91:173–84.
[67] Mezzetti M, G. IJ. Bayesian inference for the Cox model using correlated gamma process priors. Technical report, Dpt of Biostatistics, Harvard School of Public Health; 2000.
[68] James L. Bayesian calculus for gamma processes with applications to semi-parametric intensity models. Sankhy 2003;65:179–206.
[69] Nieto-Barajas LE WS. Markov beta and gamma processes for modelling hazard rates. Scand J Stat 2002;29:413–24.
[70] Chatzis S, Korkinof D, Y. D. A spatially-constrained normalized gamma process for data clustering. In: Artificial intelligence applications and innovations, IFIP advances in information and communication technology, vol. 381. 2012, p. 337–46.
[71] An D, Choi J-H, Kim NH. Prognostics 101: A tutorial for particle filter-based prognostics algorithm using matlab. Reliab Eng Syst Saf 2013;115:161–9.
[72] Liu Y. Adaptive just-in-time and relevant vector machine based soft-sensors with adaptive differential evolution algorithms for parameter optimization. Chem Eng Sci 2017;172:571–84.
[73] Liu Y, Guo J, Wang Q, Huang D. Prediction of filamentous sludge bulking using a state-based Gaussian processes regression model. Sci Rep 2016;6(1):1–11.